Ultrafast nonthermal NV center formation in diamond

Marie Kempkes[a], Tobias Zier[a], Kilian Singer[b], Martin E. Garcia[a,*]

[a] *Theoretische Physik, Universität Kassel and Center for Interdisciplinary Nanostructure Science and Technology (CINSaT), Heinrich-Plett-Str. 40, 34132 Kassel, Germany*
[b] *Experimentalphysik I, Institut für Physik, Universität Kassel, Heinrich-Plett-Straße 40, 34132 Kassel, Germany*

Abstract

NV color centers in diamond exhibit a variety of interesting properties which make them suitable for different technological applications, like quantum sensing, secure message encryption and biological imaging. They can also be used as qubits. In order to construct arrays of NV centers for quantum computing, it is necessary to maximize interqubit interactions and, at the same time, minimize all sources of decoherence. This could possibly be achieved by using femtosecond-laser pulses in the production process. In this work, we performed ab initio atomistic simulations to study ultrafast nonthermal NV center formation in diamond induced by excitation through femtosecond-laser pulses. Our results indicate that the interatomic bonding properties can be modified by the excitation in such a way that a vacancy and a nitrogen impurity, initially not nearest neighbors, attract themselves and form a NV center within 250 fs after the excitation. In contrast to the thermal behavior, here, the nitrogen atom starts to oscillate nonthermally between two grid points after the excitation. For comparison to the thermal case we performed a single run in which a NV center is thermally formed at $T = 1500$ K in one of our supercells.

Keywords: NV color center formation, femtosecond-laser pulses, nonthermal conditions, ultrafast crystal response, ab initio molecular dynamics simulations, NV centers in diamond

*Corresponding author: Martin E. Garcia, m.garcia@uni-kassel.de, +49 561 804-4480
Email addresses: Marie.kempkes@outlook.de (Marie Kempkes), zier@uni-kassel.de (Tobias Zier), ks@uni-kassel.de (Kilian Singer)

1. Introduction

The development of reliable and stable quantum computers is expected to revolutionize almost any activity in the world. With the help of the superposition principle and quantum entanglement, processors composed of qubits can solve problems which are impossible to handle by classical computers. Nitrogen-vacancy (NV) centers in diamond have recently emerged as one of the most suitable candidates for representing qubits [1]. Especially, their important role in recent successfully performed quantum simulations is remarkable and promising [2]. In addition, they can be used as quantum sensors of magnetic fields of a few nanotesla [3, 4, 5] and electric fields [6] or act as single photon emitters for quantum cryptography [7]. Besides the quantum applications, NV centers in diamond are also used as biomarkers for tracking biological processes since diamond is compatible with living cells [8].

In an ideal situation NV centers are deterministically created at defined distances in an isotopically pure diamond substrate. Their nuclear spins can then be used as long lived qubits and allow for repetitive readout [9] such that fidelity quantum devices are feasible. To assure that, production techniques should provide a deterministic high quality generation of NV centers. For that reason, their manufacturing process is of current fundamental interest [10]. In general, it consists of the implantation of the color center components into the diamond environment and the merging of the components, so that NV centers can be formed. The implantation step is mainly realized by ion bombardment of the target diamond crystal [11, 12], deterministic single ion implantation [13, 14] or by insertion during the diamond crystal growth process [15]. By using analytical potential molecular dynamics (classical MD), insights into the nitrogen implantation by ion bombardment in diamond can be obtained [16]. However, the uncertainty in the depth distribution and possible occurring local lattice deformations could potentially affect the coherence time. The insertion of nitrogen atoms during crystal growth could produce NV centers with nanometer accuracy

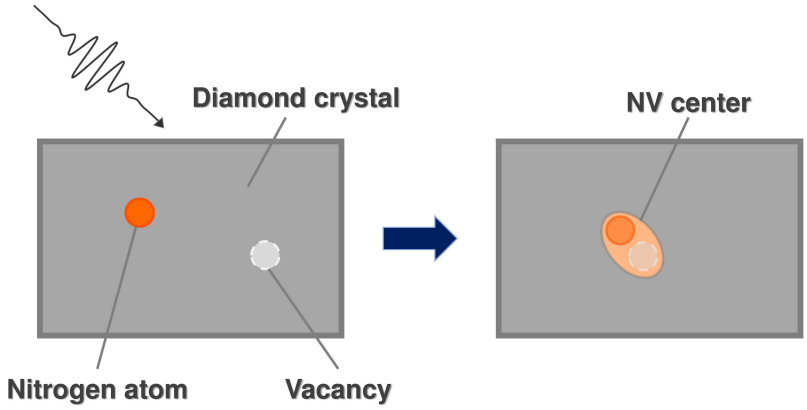

Figure 1: Schematic illustration of the femtosecond-laser induced nonthermal NV center formation in diamond. The laser energy is used to merge the initially separated nitrogen atom with the crystal vacancy with low impact on the surrounding crystal.

and without additional lattice deformations. But other nitrogen defects occur during the growth process, like, N_3, N^+ or interstitial nitrogen defects [17]. Unfortunately, during the implantation process only a very small number of NV centers is directly created, more or less by accident. Usually, both techniques produce nitrogen atoms and crystal vacancies, which are well separated in the diamond crystal. Therefore, after the implantation a second step is needed to gain a relatively high and homogeneously distributed NV center density. In general, this is done by thermal annealing. Due to the thermal heating of the crystalline system the atoms gain kinetic energy, which increases their mobility, whereas the interatomic bonding is barely affected. Above a certain threshold, the kinetic energy of the nitrogen atoms and/or the vacancies is big enough to overcome the still attractive atomic bonding and start to diffuse through the host crystal until they become neighbors. In this vicinity they could merge into the energetically very stable NV center configuration. The ensuing cooling of the whole crystal then solidifies the NV center distribution.

Very recently, tight binding methods were used to simulate the thermal an-

nealing process in order to optimize it with respect to heating temperature and heating duration [18]. Instead of using thermal heating, we propose to induce a nonthermal formation of color centers providing the necessary formation energy by ultrashort laser pulses (see fig. 1). The fact that femtosecond-laser pulses can directly access the bonding properties of the solid without disturbing the atomic system directly makes them an ideal tool to address NV center formation [19] in an already implanted diamond crystal. Therefore, we simulated the femtosecond-laser pulse induced formation of a NV center in diamond by ab initio methods. Atomic snapshots in fig. 4 of our results indicate, as a proof of concept, that femtosecond-laser pulses could be used to controllably produce NV centers nonthermally on a timescale less than 250 fs. In addition, we could resolve the underlying mechanisms by following the atomic pathways after the excitation.

2. Theory and simulations

In contrast to thermal heating, in which every degree of freedom in the electronic and the atomic system gets the same amount of energy, femtosecond-laser pulses deposit most of their energy in the electronic system. Coincidentally, the atomic system gains nearly no energy from the excitation directly. The interaction of laser photons with the electronic system results in a nonthermal distribution of occupied electronic states. However, due to fast thermalization processes, which are faster than any structural changes, it is reasonable to assume that the electrons quickly reach a thermal distribution $n_{i,\vec{k}}$ with a common electronic temperature T_e after the excitation. Intense femtosecond-laser pulses can easily induce electronic temperatures of several 10 000 K. The resulting changes in the electronic occupation after such intense excitations have a direct influence on the material properties. In materials, like, silicon and diamond, electrons are excited to a high portion from bonding into anti-bonding states [20], which weakens or softens the interatomic bonding [21]. As a consequence of the changed bonding, forces appear on the atoms, which accelerate them away

from their initial positions and produce ultrafast crystal responses that are not obtainable in thermal equilibrium. A sufficient way to account for this bond changes and the ensuing additional forces is the concept of a multidimensional potential energy surface (PES). In the case of a laser-induced nonzero electronic temperature the electronic free energy F_e has to be used to describe the PES in the framework of a generalized Born-Oppenheimer approximation. Thus, the PES reads

$$F_e(\{\vec{R}_i\}, t) = \sum_{i,\vec{k}} n_{i,\vec{k}} \cdot \epsilon_i(\vec{k}) + V_{\mathrm{II}}(\{\vec{R}_i\}) - T_e(t) \cdot S_e(t) \ , \tag{1}$$

where $\epsilon_i(\vec{k})$ are the eigenvalues of the electronic system, $V_{\mathrm{II}}(\{\vec{R}_i\})$ describes the interaction between the ions and $S_e(t)$ is the electronic entropy. Here, we use the laser-induced electronic temperature and its resulting changes in the bonding properties to force nonthermal NV center formation. This is in two ways advantageous. First, the atomic mobility is increased by the appearing forces. Second, the interatomic barriers are lowered, which makes it easier for the atoms to jump to the next lattice site. For sufficiently intense femtosecond-laser pulses interatomic bondings could even break, so that the bonding barrier disappears.

In order to resolve the atomic pathways during the femtosecond-laser induced nonthermal formation of a NV centers in diamond we performed ab initio molecular dynamics (MD) simulations using our in-house code CHIVES (For more detailed description see Sec. 5). The excitation is simulated by a raise of the electronic temperature at every simulation step according to an inverse error function that corresponds to a Gaussian pulse with a FWHM of 50 fs, until the maximum temperature of $T_e = 47\,366.6$ K is reached. At this high electronic temperature $n = 11.4\%$ of valence electrons is excited. Using the Drude formula for a laser wavelength of 620 nm a laser fluence of $3.382\ \frac{\mathrm{J}}{\mathrm{cm}^2}$ [22] is needed. Note that this fluence can produce damage of the structure on longer times. We point out that the purpose of this investigation is to get proof of principle.

In the presented work, we used a cuboid simulation cell of diamond with a

volume of 1596 Å^3 or 1.596 nm^3, respectively. Ideally, without crystal defects, $N = 288$ carbon atoms would fit in. In order to study laser-induced ultrafast formation of a NV center one randomly assigned carbon atom was substituted by a nitrogen atom. The vacancy was implanted in the crystal by removing one carbon atom in the surrounding of the nitrogen atom, but not a nearest neighbor one. Due to the crystal impurities the crystal configuration is no longer in equilibrium. We therefore relaxed the system [23] before we thermalized it by an Andersen thermostat to $T = 300$ K. Out of the thermalization we extracted 20 independent initial conditions for our MD simulation runs, which last in total 600 fs. Note, that the vacancy and the nitrogen atom are located near the same lattice sites in each run, but have different initial displacements and velocities. The shown quantities are averaged over 20 runs, if not indicated differently.

To analyze the structure of the crystal after laser excitation we calculated the time evolution of the root mean square atomic displacement $rmsd(t)$. It is defined by

$$rmsd(t) = \sqrt{\frac{1}{N}\sum_{i=1}^{N}(\vec{r}_i(t) - \vec{r}_{0,i})^2}\ , \tag{2}$$

where N is the total number of atoms in the used supercell. $\vec{r}_{\mathrm{i}}(t)$ is the position of the i-th atom at time t. As reference we used $\vec{r}_{0,\mathrm{i}}$ of the ideal crystal at $T = 0$ K. The $rmsd$ value is an averaged quantity over the whole used supercell and could not give specific insights into particular microscopic atomic pathways. In order to resolve those pathways we computed specific atomic distances (see fig. 5). In particular, we computed the distance of the interstitial carbon atom to its nearest initial grid point of the ideal diamond crystal $r^C(t)$. Furthermore, we calculated the time-dependent distance of this carbon atom to the neighboring grid point of the vacancy. The same was done for the nitrogen impurity with respect to its initial grid point and the grid point of the interstitial carbon atom.

3. Results and discussion

Diamond is an extremely stable crystalline structure with a large band gap E_{gap} of around 5.47 eV [24]. In CHIVES, we obtain a value of $E_{\mathrm{gap}} = 4.20$ eV.

This discrepancy is mainly caused by the local density approximation (LDA) that is used for the exchange-correlation functional in CHIVES. It is known that LDA underestimates the electronic band gap in contrast to, e.g., hybrid functionals. However, we like to note that our value is in good agreement with other LDA computations that obtained a value of 4.11 eV [25]. Since the band structure is sufficiently well described by LDA, our results would only change quantitatively and not qualitatively by using different methods that give a value more related to the experimental value of the band gap. In particular, only the excitation strength would increase to see the same effects. However, an intense femtosecond-laser excitation is needed to induce nonthermal bond changes in diamond, which are caused by electrons excited above the band gap. We believe that the optimal wavelengths for the nonthermal manipulation of NV centers in diamond should lie in the UV regime, which does not need a high number of photons to excite electrons to the conduction band. Lower laser frequencies would need very high intensities in order to allow for multi photon processes to overcome the band gap, thus producing not desired damage on the sample.

As a consequence of the large possible excitation intensity range it becomes even more difficult to narrow down the laser-intensity range that induces predominantly a particular phenomenon. Since ab initio MD simulations are expensive in computation time it was necessary to find the possible excitation regime for nonthermal NV center formation by static computations. Using the method of frozen phonons we calculated the potential free energy surface in particular crystal directions (see fig. 2). The potential barrier for a carbon atom embedded in the diamond crystal next to a nitrogen atom and a vacancy (fig. 2 (a) and (b)) is lowered by 1.35 eV and shifted by 0.0786 Å to higher displacements compared to the ground state for an induced electronic temperature of $T_e = 31\,577.7$ K, which corresponds to a number of excited valence electrons of $n = 5.6\%$.

At even higher electronic temperatures the potential free energy switched completely into an attractive curve, so that the former lattice site barrier vanishes. The initial configuration is no longer energetically stable. As a conse-

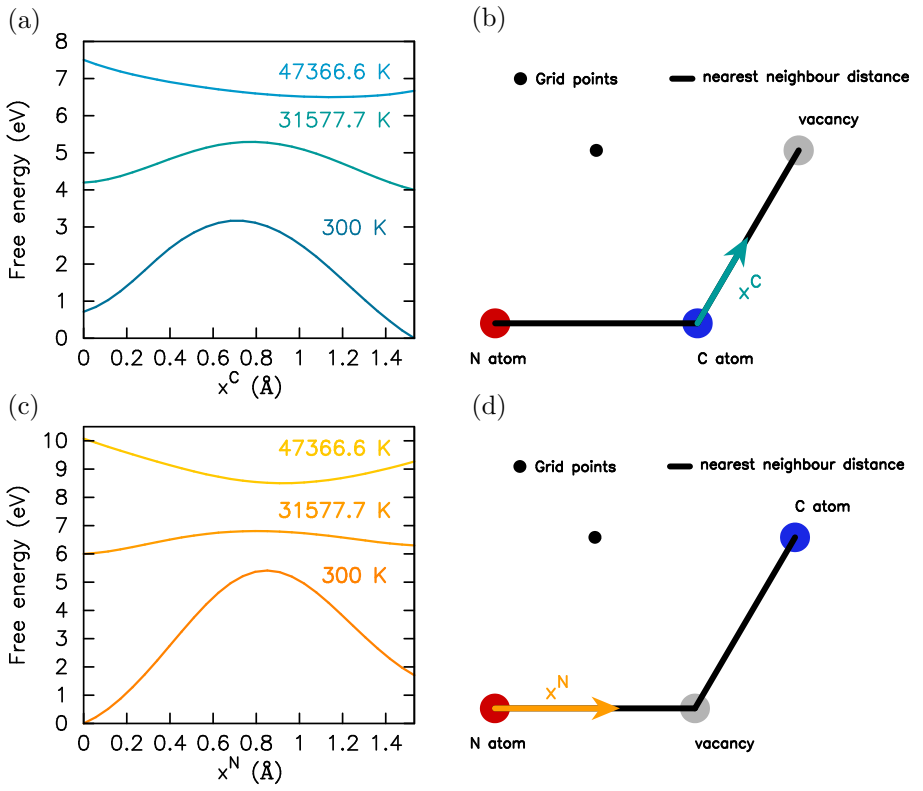

Figure 2: Static potential energy computations in particular directions.(a) Static computations of the total free energy in dependence of the atomic displacement of an interstitial carbon atom along the connection line towards the vacancy (sketch (b)) for different laser-induced electronic temperatures. (c) The same computation for a displaced nitrogen atom along the connection line that points to a vacant grid point (sketch (d)). The free energy is computed for the whole supercell and is shifted for comparability.

quence the carbon atom would interchange positions with the vacancy. We used the same procedure for a diamond crystal in which the nitrogen atom and the vacancy are nearest neighbors (fig. 2 (c) and (d)). It can be seen that once the NV center is build it is extremely stable in a ground state diamond crystal. Nevertheless, the free energy becomes attractive on the direction line between the lattice sites of the nitrogen atom and the vacancy at $T_e = 47\,366.6$ K. We like to note, that the made static computations in only one particular direction are not sufficient enough to predict the complex atomic motion on the high dimension potential energy surface. The success of producing NV centers by

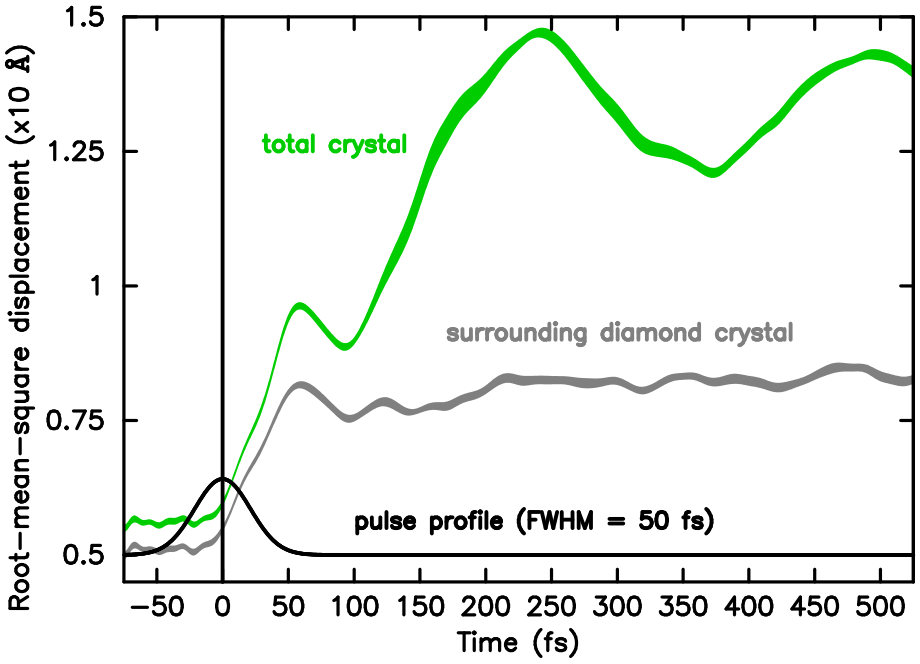

Figure 3: Averaged root-mean-square atomic displacement as a function of time for the whole simulation cell (green). As reference the root-mean-square displacement of the surrounding diamond crystal is shown, which excludes the contributions of the carbon atoms between the vacancy and the nitrogen atom and of the nitrogen atom itself (grey). $t = 0$ is calibrated to the maximum of the used Gaussian femtosecond-laser pulse with a FWHM of 50 fs (black solid). The width of the curves indicate twice the standard deviation.

thermal annealing (see fig. 6) confirms that less heat is needed than the here computed static barrier computation suggests. Therefore, it is mandatory to consider phonon motions and atomic collision, which allow atomic trajectories that could overcome or circumvent the potential barrier present in the direct connection line used in fig. 2. By performing parameter-free MD simulations at the excitation strength obtained from the static computations of the PES all these effects are included. Fig. 3 shows the time evolution of the root-mean-square atomic displacement $rmsd(t)$ for the used supercell and a laser-induced electronic temperature of $T_e = 47\,366.6$ K. Due to the large band gap of diamond the crystal does not start to react before the maximum of the pulse.

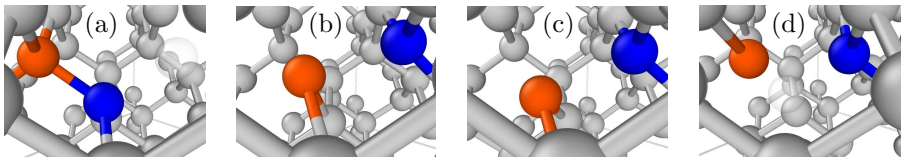

Figure 4: Closeups of our simulation cell near the nitrogen impurity (orange) and the crystal vacancy (transparent). (a) The initial ground state configuration at $T_e = 300$ K before the femtosecond-laser excitation. The nitrogen atom and the vacancy (right upper quadrant) are not nearest neighbours. (b) $t = 165$ fs after the laser excitation, which induces an electronic temperature of $T_e = 47366.6$ K, the interstitial carbon atom (blue) changes the lattice site with the vacancy. (c) $t = 245$ fs, the nitrogen atom followed the motion of the interstitial carbon atom. (d) At $t = 265$ fs the nitrogen atom has moved back near its initial position and the vacancy occupies the initial carbon lattice site. [26].

By comparing the *rmsd* of the whole crystal to the pure surrounding, in which the colored atoms of fig. 4 are not considered, it becomes obvious that those atoms gain a very high mobility after the femtosecond-laser pulse. The *rmsd* of the surrounding is almost doubled when considering those atoms. In order to reveal the atomic pathways during and after the excitation we computed relative distances of the nitrogen atom and the interstitial carbon atom to defined lattice grid points (sketch in fig. 5 (a)). Within 200 fs after the maximum of the exciting pulse, the interstitial carbon atom interchanges its position with the vacancy (fig. 5 (c)). The sum of $r^C(t)$, which measures the distance to the initial grid point at $T = 0$ K, and the distance to the initial vacancy grid point is slightly larger than the nearest neighbor distance in diamond, which indicates that not the direct path is used by the moving atom. Nevertheless, the carbon atom seems to be tightly bonded to the surrounding diamond crystal after the transition, since it stays close to its new lattice grid point. Triggered by the oscillation of the carbon atom at around $t = 75$ fs, the nitrogen atom starts slowly to follow the carbon atom (see fig. 5 (b)). Instead of moving straight to the neighboring vacant grid point of the moved carbon atom, the nitrogen atom oscillates around 0.78 Å, which is close to 0.9 Å, the minimum of the static calculated potential in fig. 2. The discrepancy is mainly caused by the laser-induced nonthermal atomic motion of the surrounding as well as partially

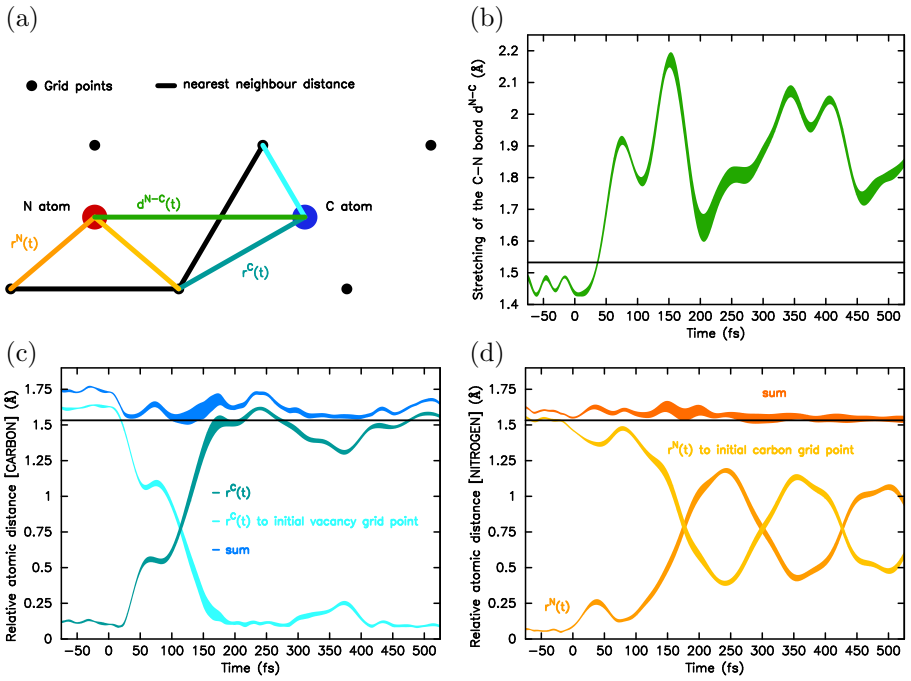

Figure 5: Relative atomic distances for selected atoms and grid points. (a) Sketch of the relative atomic distances of the nitrogen atom and the interstitial carbon atom for an arbitrary time after the femtosecond-laser excitation. The color coding is used in the following graphs. The horizontal black line indicates the distance between grid points in the diamond crystal, here 1.5325 Å. (b) Interatomic distance between the interstitial carbon atom and the nitrogen impurity as a function of time. (c) Time evolution of the relative atomic distance of the carbon atom to its initial grid point $r^C(t)$ (turquoise), to the initial vacancy grid point (light blue) and the sum of both distances (blue) for a laser induced electronic temperature of $T_e = 47\,366.6$ K. About 150 fs after laser excitation the carbon atom is located close to the initial grid point of the vacancy. (d) Relative atomic distance of the nitrogen atom to its initial grid point (light orange), to the initial carbon grid point (yellow) and the sum of both distances (orange).

by the initial ionic motion at $T = 300$ K. However, the initial grid points seem to be no longer energetic minima in the laser-excited state. The shifted energy minimum due to the laser-excitation changes significantly the configuration of the NV center in the crystal and therefore its properties, which opens the field for customer designed NV centers by femtosecond-laser pulses. Nonetheless, the configuration of the NV center near the grid points could be obtained by fast cooling of the sample after the NV formation. Moreover, it could be benefi-

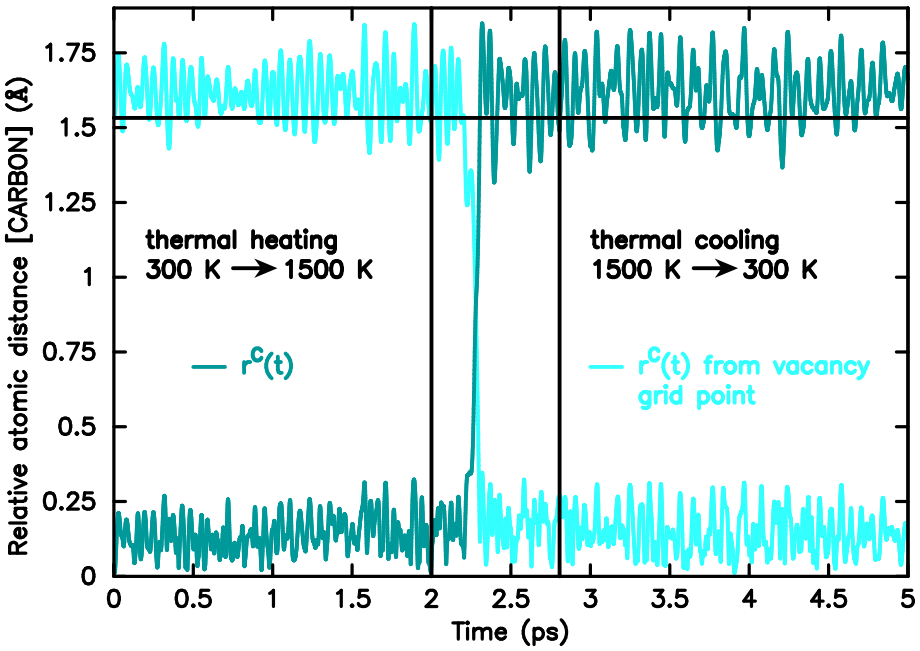

Figure 6: Time dependence of the relative atomic distance of the carbon atom for a particular thermal annealing run. The same color coding as in fig. 5 is used. Thermal heating of the crystal to 1500 K provides enough energy for the interstitial carbon atom to interchange its position with the vacancy. The ensuing cooling to 300 K does not reverse the configuration.

cial to use a moderate laser-excitation, which does not flip the potential energy surface completely but lowers the potential barrier sufficiently, so that a small heat increase could provide enough energy to overcome it. A thermal annealing run of the same simulation cell in CHIVES showed that heating the system to around 1500 K provides enough thermal energy that the interstitial carbon atom can interchanges its position with the vacancy so that a stable NV center can be formed (fig. 6). The ensuing cooling of the system does not reverse this formation, it instead solidifies it. We like to note, that recently performed tight-binding MD simulations indicate that less thermal energy is needed for the NV center to form [18]. However, the formation process then takes several nanoseconds instead of picoseconds as in our case (fig. 6).

4. Summary and Outlook

In conclusion, we simulated a femtosecond-laser induced NV center formation in a diamond environment using electronic-temperature-dependent DFT. Our parameter-free MD simulations show that the formation process takes place on an ultrafast timescale of 250 fs after the excitation. This laser-driven nonthermal formation process of a NV center will only take place if the nitrogen atom and the vacancy are located close to each other. It is essential for the formation process that the vacancy detects an anisotropic bonding in the direction of the nitrogen atom caused by the latter one. Then it is energetically favourable to move towards the nitrogen atom. In addition, the laser-induced interatomic bonding changes cause an oscillatory behavior of the nitrogen atom, which is in contrast to the thermal case in which the nitrogen atom remains usually near a grid point. Our static computations reveal that the diamond grid points do not longer correspond to a minimum in the PES at the used high excitation. In addition, those computations indicate that the energy minimum that defines the NV center configuration is changed in dependence of the laser strength. This could possibly be used to produce customer designed NV centers with different properties. However, we have to mention that the electronic temperature used in this work is extremely high and could produce damage at longer times. Therefore, at the moment we can only present a proof of concept that it is possible to nonthermally manipulate the vacancies and N ions to form a NV center. A fine tuning considering lower intensities and different pulse durations must follow. Another natural follow-up of this study can be to simulate larger systems over longer time scales, which would also cover the description of nanodiamonds [27]. Since ab-initio simulations are restricted to cells of less than 1000 atoms, one can scale up the systems by constructing electronic-temperature dependent interatomic potentials, using the method described in ref. [28]. In this way, one can be able to describe large simulation cells with an open surface, making possible the simulation of laser-induced creation and manipulation of vacancies and NV centers. Particularly interesting, due to their applications, is the case of

creation of NV centers in nanodiamonds with functional groups on the surface. In addition, such large scale simulation would make it possible to simulate the creation as well as the diffusion of vacancies in diamond.

5. Appendix: Code for Highly excIted Valence Electron Systems (CHIVES)

In order to resolve the atomic pathways during the femtosecond-laser induced nonthermal formation of a NV centers in diamond we performed ab initio MD simulations using our in-house code CHIVES [29, 30, 31] is a density-functional-theory code that is extended to nonzero electronic temperatures using the functionals derived by Mermin [32]. In order to describe femtosecond-laser excitations of solids by those functionals, it is assumed that the electronic system equilibrates faster than structural changes appear and adapts quickly a Fermi distribution of a specific electronic temperature, which corresponds to the absorbed energy. In such cases the laser-excitation is completely defined by the electronic temperature.

Since incoherent electron-phonon interactions are not considered here, this temperature will stay constant throughout the remaining simulation. CHIVES computes on the fly at every simulation step the potential energy surface (PES) defined by the electronic temperature and the actual atomic positions. Laser-induced changes in the interatomic forces, which produce ultrafast structural changes, can now directly be computed from the PES. Although, the computation time becomes very expensive if the structural symmetry is lost due to ultrafast laser-induced phenomena, CHIVES enables to use supercells containing up to 1440 atoms in reasonable time [33]. The high simulation speed is mostly attributed to the highly hybrid parallelization of several subroutines, the use of order N methods, if applicable, and the subdivided description of the electronic system. Tightly bonded core electrons are represented by norm-conserving pseudopotentials. For the valence electrons of the system atom-centered Gaussian basis sets are used. This reduces the number of basis states for carbon to 21

[34]. For nitrogen 25 basis states are needed [35].

Acknowledgements

Computations were performed at the Lichtenberg High Performance Computer of the Technical University Darmstadt. Financial support of the Deutsche Forschungsgemeinschaft through the project GA465/15-2 is gratefully acknowledged.

References

[1] L. Childress, R. Hanson, Diamond nv centers for quantum computing and quantum networks, MRS Bulletin 38 (2) (2013) 134–138. doi:10.1557/mrs.2013.20.

[2] M. V. G. Dutt, L. Childress, L. Jiang, E. Togan, J. Maze, F. Jelezko, *et al.*, Quantum register based on individual electronic and nuclear spin qubits in diamond, Science 316 (5829) (2007) 1312–1316. doi:10.1126/science.1139831.

[3] J. R. Maze, P. L. Stanwix, J. S. Hodges, S. Hong, J. M. Taylor, P. Cappellaro, *et al.*, Nanoscale magnetic sensing with an individual electronic spin in diamond, Nature 455 (2008) 644–647. doi:https://doi.org/10.1038/nature07279.

[4] P. Tsai, O. Y. Chen, Y. Tzeng, Y. Hui, J. Guo, C. Wu, *et al.*, Gold/diamond nanohybrids for quantum sensing applications, EPJ Quantum Technol. 2 (19). doi:https://doi.org/10.1140/epjqt/s40507-015-0031-3.

[5] J. M. Boss, K. S. Cujia, J. Zopes, C. L. Degen, Quantum sensing with arbitrary frequency resolution, Science 356 (6340) (2017) 837–840. doi:10.1126/science.aam7009.

[6] F. Dolde, H. Fedder, M. Doherty, T. Nöbauer, F. Rempp, G. Balasubramanian, *et al.*, Electric-field sensing using single diamond spins, Nature Phys. 7 (2011) 459–463. doi:https://doi.org/10.1038/nphys1969.

[7] A. Beveratos, R. Brouri, T. Gacoin, A. Villing, J.-P. Poizat, P. Grangier, Single photon quantum cryptography, Phys. Rev. Lett. 89 (2002) 187901. doi:10.1103/PhysRevLett.89.187901.

[8] Y. Chang, H. Lee, K. Chen, C. Chang, D. Tsai, C. Fu, *et al.*, Mass production and dynamic imaging of fluorescent nanodiamonds, Nature Nanotech 3 (2008) 284–288. doi:https://doi.org/10.1038/nnano.2008.99.

[9] L. Jiang, J. S. Hodges, J. R. Maze, P. Maurer, J. M. Taylor, D. G. Cory, P. R. Hemmer, R. L. Walsworth, A. Yacoby, A. S. Zibrov, M. D. Lukin, Repetitive readout of a single electronic spin via quantum logic with nuclear spin ancillae, Science 326 (2009) 267–272. doi:10.1126/science.1176496.

[10] J. M. Smith, S. A. Meynell, A. C. Bleszynski Jayich, J. Meijer, Colour centre generation in diamond for quantum technologies, Nanophotonics 8 (11) (2019) 196.

[11] F. C. Waldermann, P. Olivero, J. Nunn, K. Surmacz, Z. Wang, D. Jaksch, *et al.*, Creating diamond color centers for quantum optical applications, Diamond & Related Materials 16 (2007) 1887–1895. doi:https://doi.org/10.1016/j.diamond.2007.09.009.

[12] B. Naydenov, V. Richter, J. Beck, M. Steiner, P. Neumann, G. Balasubramanian, *et al.*, Enhanced generation of single optically active spins in diamond by ion implantation, Applied Physics Letters 96 (16) (2010) 163108. doi:10.1063/1.3409221.

[13] G. Jacob, K. Groot-Berning, S. Wolf, S. Ulm, L. Couturier, S. T. Dawkins, U. G. Poschinger, F. Schmidt-Kaler, K. Singer, Transmission microscopy with nanometer resolution using a deterministic single ion source, Phys. Rev. Lett. 117 (2016) 043001.

[14] K. Groot-Berning, T. Kornher, G. Jacob, F. Stopp, S. T. Dawkins, R. Kolesov, J. Wrachtrup, K. Singer, F. Schmidt-Kaler, Deterministic single-ion implantation of rare-earth ions for nanometer-resolution color-center generation, Phys. Rev. Lett. 123 (2019) 106802.

[15] M. A. Lobaev, A. M. Gorbachev, S. A. Bogdanov, A. L. Vikharev, D. B. Radishev, V. A. Isaev, *et al.*, Nv-center formation in single crystal diamond at different cvd growth conditions, physica status solidi (a) 215 (22) (2018) 1800205. doi:10.1002/pssa.201800205.

[16] O. Lehtinen, B. Naydenov, P. Börner, K. Melentjevic, C. Müller, L. McGuinness, *et al.*, Molecular dynamics simulations of shallow nitrogen and silicon implantation into diamond, Phys. Rev. B 93 (2016) 035202. doi:10.1103/PhysRevB.93.035202.

[17] R. Rubinas, V. V. Vorobyov, V. V. Soshenko, S. V. Bolshedvorskii, V. N. Sorokin, A. N. Smolyaninov, *et al.*, Spin properties of NV centers in high-pressure, high-temperature grown diamond, Journal of Physics Communications 2 (11) (2018) 115003. doi:10.1088/2399-6528/aae992.

[18] M. O. Smirnova, Formation of nitrogen-vacancy centres in diamond: tight-binding molecular dynamic simulation, Journal of Physics: Conference Series 1435 (2020) 012069. doi:10.1088/1742-6596/1435/1/012069.

[19] Y.-C. Chen, B. Griffiths, L. Weng, S. S. Nicley, S. N. Ishmael, Y. Lekhai, S. Johnson, C. J. Stephen, B. L. Green, G. W. Morley, M. E. Newton, M. J. Booth, P. S. Salter, J. M. Smith, Laser writing of individual nitrogen-vacancy defects in diamond with near-unity yield, Optica 6 (5) (2019) 662–667.

[20] P. L. Silvestrelli, M. Parrinello, Ab initio molecular dynamics simulation of laser melting of graphite, Journal of Applied Physics 83 (5) (1998) 2478–2483. doi:10.1063/1.366989.

[21] P. Stampfli, K. H. Bennemann, Theory for the instability of the diamond structure of si, ge, and c induced by a dense electron-hole plasma, Phys. Rev. B 42 (1990) 7163–7173. doi:10.1103/PhysRevB.42.7163.

[22] H. O. Jeschke, M. E. Garcia, K. H. Bennemann, Theory for the ultrafast ablation of graphite films, Phys. Rev. Lett. 87 (2001) 015003. doi:10.1103/PhysRevLett.87.015003.

[23] E. Bitzek, P. Koskinen, F. Gähler, M. Moseler, P. Gumbsch, Structural relaxation made simple, Phys. Rev. Lett. 97 (2006) 170201. doi:10.1103/PhysRevLett.97.170201.

[24] C. J. H. Wort, R. S. Balmer, Diamond as an electronic material, Materials Today 11 (1) (2008) 22 – 28. doi:https://doi.org/10.1016/S1369-7021(07)70349-8.

[25] H. Löfås, A. Grigoriev, J. Isberg, R. Ahuja, Effective masses and electronic structure of diamond including electron correlation effects in first principles calculations using the gw-approximation, AIP Advances 1 (3) (2011) 032139. doi:10.1063/1.3630932.

[26] A. Stukowski, Visualization and analysis of atomistic simulation data with OVITO-the Open Visualization Tool, MODELLING AND SIMULATION IN MATERIALS SCIENCE AND ENGINEERING 18 (1). doi:{10.1088/0965-0393/18/1/015012}.

[27] A. H. Romero, H. O. Jeschke, M. E. Garcia, Laser manipulation of nanodiamonds, Computational Materials Science 35 (3) (2006) 179 – 182. doi:https://doi.org/10.1016/j.commatsci.2004.09.051.

[28] B. Bauerhenne, V. P. Lipp, T. Zier, E. S. Zijlstra, M. E. Garcia, Self-learning method for construction of analytical interatomic potentials to describe laser-excited materials, Phys. Rev. Lett. 124 (2020) 085501. doi:10.1103/PhysRevLett.124.085501.

[29] E. S. Zijlstra, A. Kalitsov, T. Zier, M. E. Garcia, Fractional diffusion in silicon, Adv. Mater. 25 (39) (2013) 5605–5608. doi:10.1002/adma201302559.

[30] T. Zier, E. S. Zijlstra, M. E. Garcia, Quasimomentum-space image for ultrafast melting of silicon, Phys. Rev. Lett. 116 (2016) 153901. doi:10.1103/PhysRevLett.116.153901.

[31] T. Zier, E. S. Zijlstra, S. Krylow, M. E. Garcia, Simulations of laser-induced dynamics in free-standing thin silicon films, Appl. Phys. A 123 (10) (2017) 625. doi:10.1007/s00339-017-1230-9.

[32] N. D. Mermin, Thermal properties of the inhomogeneous electron gas, Phys. Rev. 137 (1965) A1441–A1443. doi:10.1103/PhysRev.137.A1441.

[33] L. Waldecker, T. Vasileiadis, R. Bertoni, R. Ernstorfer, T. Zier, F. Valencia, *et al.*, Coherent and incoherent structural dynamics in laser-excited antimony, Phys. Rev. B 95 (5) (2017) 054302. doi:10.1103/PhysRevB.95.054302.

[34] E. Zijlstra, T. Zier, B. Bauerhenne, S. Krylow, P. Geiger, M. Garcia, Femtosecond-laser-induced bond breaking and structural modifications in silicon, tio2, and defective graphene: An ab initio molecular dynamics study, Applied Physics A 114. doi:10.1007/s00339-013-8080-x.

[35] B. Bauerhenne, E. S. Zijlstra, A. Kalitsov, M. E. Garcia, Mechanical properties of boron-nitride nanotubes after intense femtosecond-laser excitation, Nanotechnology 25 (14) (2014) 145701. doi:10.1088/0957-4484/25/14/145701.